Langmuir

Article

pubs.acs.org/Langmuir

Nanoscale Ion Sequestration To Determine the Polarity Selectivity of Ion Conductance in Carriers and Channels

Charles G. Cranfield,*[,†] Taren Bettler,[‡] and Bruce Cornell[‡]

[†]School of Medical and Molecular Biosciences, University of Technology Sydney, PO Box 123, Ultimo, NSW 2007, Australia

[‡]SDx Tethered Membranes Pty Ltd., Unit 6, 30-32 Barcoo St., Roseville, NSW 2069, Australia

ABSTRACT: The nanoscale spacing between a tethered lipid bilayer membrane (tBLM) and its supporting gold electrode can be utilized to determine the polarity selectivity of the conduction of ion channels and ion carriers embedded in a membrane. The technique relies upon a bias voltage sequestering or eliminating ions, of a particular polarity, into or out of the aqueous electrolyte region between the gold electrode and the tethered membrane. A demonstration is given, using ac swept frequency impedance spectrometry, of the bias polarity dependence of the ionophore conductance of gramicidin A, a cationic selective channel, and valinomycin, a potassium ion selective carrier. We further use pulsed amperometry to show that the intrinsic voltage dependence of the ion conduction is actually selective of the polarity of the transported ion and not simply of the direction of the ionic current flow.

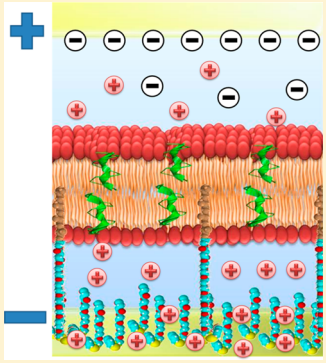

INTRODUCTION

The selectivity of a peptide or protein ion channel or carrier to the ionic polarity of the transported ion may be measured using patch clamp electrophysiology or black lipid membrane (BLM) techniques.[1,2] However, for a fragile free floating membrane the exchange of electrolyte solutions can cause damage to the membrane integrity. Similarly, the patch clamp technique depends on achieving a high impedance seal between a membrane surface and a glass pipet which can vary when changing ionic solutions of varying concentrations and compositions. We describe here a more convenient and robust alternative using a tethered bilayer lipid membrane (tBLM)[3,4] to demonstrate the cation selectivity of two of the best characterized ionophores: the cation specific *peptide gramicidin* A (gA) ion channel and the potassium specific carrier *valinomycin* (Val).

The effect arises from the nanoscale dimensions (2−2.5 nm) of the space between the membrane and the tethering gold electrode, termed here a reservoir, for ions traversing the membrane. At these small dimensions the relative concentration of ions within the reservoir may be controlled by an applied bias potential between the tethering gold electrode and the distant (100 μm) gold counter electrode.[5] Positive bias potential gradients will attract anions and repulse cations, altering the ionic concentration ratio within the reservoir to favor anions. Negative bias potential gradients will attract cations and repulse anions within the reservoir This technique is defined here as *reservoir ion sequestration* (RIS).

As described previously,[6] immediately following the application of the voltage step across the assembled membrane cartridge, a major fraction of the voltage will appear across the smallest capacitance, $C_m \sim 1\ \mu F\ cm^{-2}$ (Figure 1C), and an order of magnitude smaller fraction across the next largest capacitance, $C_{th} \sim 10\ \mu F\ cm^{-2}$, and yet a further order of magnitude smaller fraction across the largest capacitance, $C_c \sim 100\ \mu F\ cm^{-2}$. After a time, determined by the series combination of C_{th} and C_c being charged through the nonspecific bilayer conductance, G_b, plus any conductance due to G_i, the voltage across the membrane will have decayed to near zero. At this time the voltage across C_{th} and C_c will have risen to near V_{dc}. Given the relative magnitudes of C_{th} and C_c, the major fraction of the residual applied potential, V_{dc}, will reside across C_{th} indefinitely. Provided the gold surface is of high purity and the voltage is kept well below the gold oxidation potential of approximately 0.9 V, the conductive bypass at C_{th} and C_c is essentially zero.

As described in Figure 1B, one plate of C_{th} represents the electronic charge in the metallic gold electrode (represented by a line) and the other is the ionic distribution in the aqueous buffer of equal and opposite charge at the gold tethering surface (represented by a rectangle). Thus, a greater fixed negative charge on the metallic plate of C_{th} will result in a greater cationic concentration in the ionic solution at the tethering gold electrode and vice versa for a fixed positive potential. The nanoscale geometry of the reservoir volume, defined by the volume bounded by the inner layer of the tBLM and the tethering gold surface, not only results in the fixed electrode potential modulating the charge on C_{th} but also any local free ions in the electrolyte solution. It is this ionic solution that provides the source of ions for ion transport across the membrane. Thus, the polarity of the long term potential, V_{dc}, applied between C_c and C_{th} can control the local ionic strength of a chosen polarity of ion and thus the apparent polarity-dependent conduction of the ionophore. Because of the

Received: April 8, 2014
Revised: November 24, 2014

   dx.doi.org/10.1021/la504057z | *Langmuir* XXXX, XXX, XXX−XXX

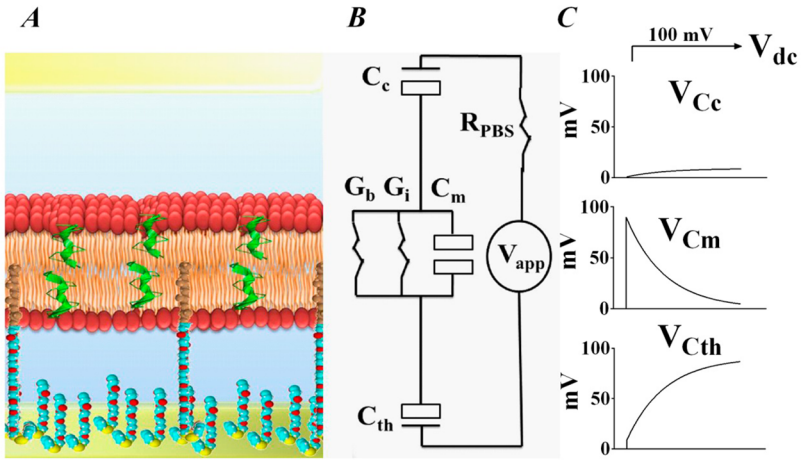

Figure 1. (A) Schematic representation of an assembled tethered membrane cartridge containing gramicidin A within a flow cell cartridge. (B) Its electrical equivalent circuit. The gold surfaces of counter electrode capacitor C_c and tethering electrode capacitor C_{th} are drawn as lines denoting the electronic charge in the metal surfaces. The opposing plates are drawn as rectangles to denote the ionic charge distributions in the solution. The membrane capacitance, C_m, is similarly represented as two rectangles representing the opposing ionic charges in the electrolyte solution at the membrane surfaces. In addition, G_b is the nonspecific bilayer conductance present in the absence of ionophore. G_i is the conductance due to the ionophore. V_{app} is the applied voltage. R_{PBS} reflects the resistance of the phosphate buffered saline (PBS). (C) A fixed potential step of V_{dc} = 100 mV is applied to the membrane, resulting in the transient voltages V_{Cc}, V_{Cm}, and V_{Cth}. As described in the text, after a brief period, V_{dc} is essentially expressed across just C_{th} (given $C_c \gg C_{th}$), and no residual voltage exists across the membrane.

restricted lateral ionic diffusion within the reservoir space, the interfacial capacitance (C_{th}) requires more than a simple capacitive term in the equivalent circuit. That is, ions being transferred across the membrane may need to diffuse laterally to evenly charge C_{th}. As previously described,[7,8] this delay in charging C_{th} results in a distributed capacitor−resistor network which may be conveniently described by incorporating a constant phase element (CPE) into the equivalent electrical circuit. The CPE possesses both a capacitive term (Q_s) and a dimensionless constant (α) which accounts for the contribution of the restricted diffusion to the capacitive phase term.

The polarity dependence of the apparent ionophore conductance, G_i, may be probed through the application of an independent low voltage ac excitation (V_{ac}) superimposed on the dc potential V_{dc}. Thus, in Figure 1B, $V_{app} = V_{dc} + V_{ac}$. If the charge on C_{th} attracts ions opposite to the polarity preference of the ionophore, the resultant current will be lower, limited by G_b and any residual nonselective ionophore conduction (G_i).

Gramicidin A is a 15 amino acid peptide derived from the soil residing bacteria *B. brevis* first isolated by Rollin Hotchkiss and René Dubos in 1939.[9] It is one of the best characterized ionophores in the scientific literature.[10,11] In lipid bilayers it forms a $\pi_{LD}^{6.3}$ right-handed β sheet helical structure anchored at the hydrocarbon−water interface by the indole N−H groups of four tryptophan residues at the C-terminus.[12−14] The conductive pathway formed by gA across lipid bilayers results from monomers within opposing leaflets forming transient dimers stabilized by six hydrogen bonds, three per monomeric gA across the bilayer and forming a nonrectifying, voltage-independent, cation selective channel with a conduction of order of pS.[15−17] These properties make gA ideally suited to engineering tBLMs with specific functionalities.[18−20] In the present study a tBLM has been formed containing gA, and the RIS technique is used to demonstrate the polarity selectivity of the gA ion channel conductance.

Valinomycin is a similarly widely studied cationic ionophore whose function, however, is dramatically different from that of the ion channel gA in that the ion transport is achieved by the

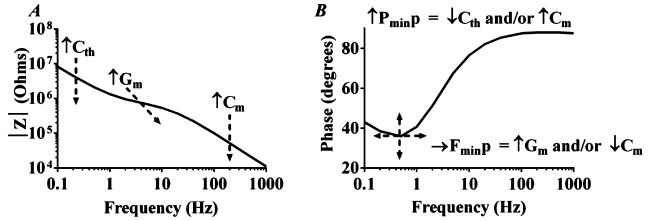

Figure 2. (A) A typical impedance versus frequency plot on a log−log scale for tBLMs. A reduction in the impedance at low frequencies is dominated by increases in C_{th}; reductions in impedance at intermediate frequencies, with a shift to higher frequencies, indicate increases in G_m; and decreases in impedances near 1 kHz are indicative of an increase in C_m. (B) A phase versus frequency profile on a linear−log scale for tBLMs. Changes in G_m and/or C_m will be reflected in shifts of the frequency at which the minimum phase occurs ($F_{min}p$), whereas changes in C_{th}/C_m are reflected in the minimum phase value itself ($P_{min}p$).

millionfold less efficient mechanism of a carrier.[21] To achieve comparable conduction, millimolar concentrations of Val are required, compared to the nanomolar concentrations of gA. Val has the additional property of being highly potassium ion (K^+) specific (10000-fold K^+ over Na^+). This specificity will be reflected in the dependence of the elements in the electrical equivalent circuit. The equivalent circuit (Figure 1B) comprising C_m, G_i, and C_{th} describes the analogous electrical circuit properties of an ion channel such as the weakly selective cationic transporter gA. We demonstrate here that for Val the equivalent circuit must additionally reflect both the properties of the K^+ transport independently of the far more concentrated Na^+ ions in solution, both of which may be probed using the RIS technique.

■ EXPERIMENTAL SECTION

tBLMs with 10% tethering lipids and 90% spacer lipids were formed using the solvent exchange technique.[6] Briefly, the procedure involves using preprepared tethered benzyl disulfide−(tetraethylene glycol)$_{n=2}$ C20-phytanyl tethers: benzyl disulfide−tetraethylene glycol−OH

dx.doi.org/10.1021/la504057z | *Langmuir* XXXX, XXX, XXX−XXX

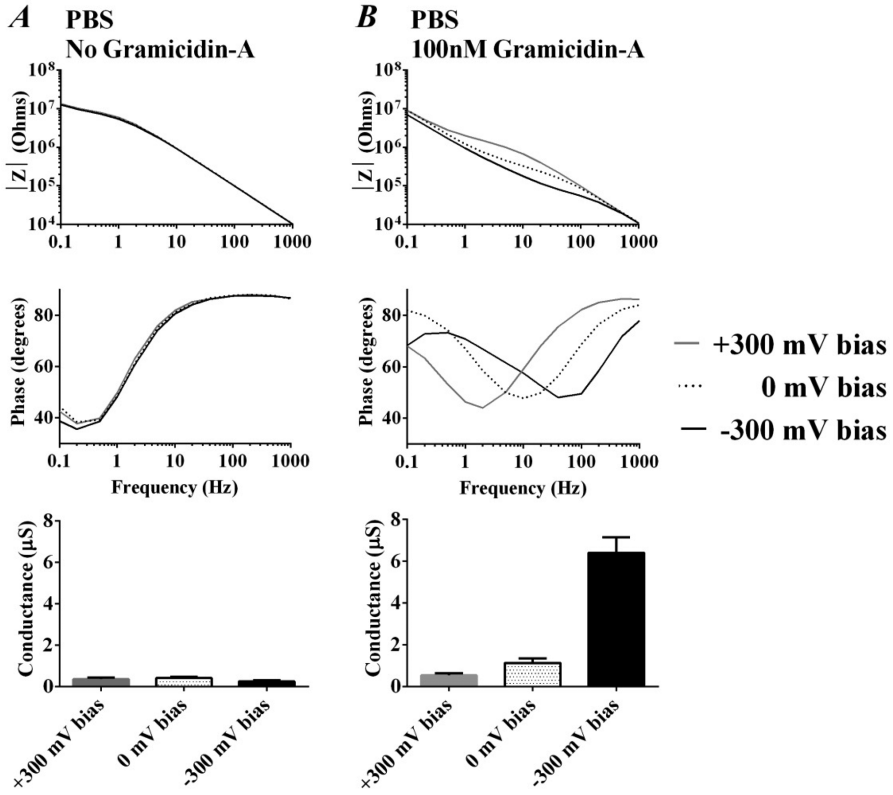

Figure 3. (A) Impedance versus frequency (top), phase versus frequency (middle), and calculated conductances (bottom) for a tBLM without gA with +300, 0, and −300 mV bias (n = 3). (B) Impedance versus frequency (top), phase versus frequency (middle), and calculated membrane conductances (G_m) (bottom) for a tBLM with 100 nM gA with +300, 0, and −300 mV bias (n = 3).

spacers in the ratio of 1:10 coated onto 2.1 mm^2 patterned, 100 nm thick fresh 5N5 gold surfaces sputter coated onto a polycarbonate slide (SDx Tethered Membranes Pty Ltd., Australia). To these tethered species, 8 μL of a 3 mM solution of a mobile lipid phase [70% zwitterionic C20 diphytanylglycerophosphatidylcholine lipid: 30% C20 diphytanyl diglyceride−OH ether] dissolved in ethanol was added via a 0.1 mm high, 1 μL volume flow cell and, after a 2 min incubation, washed with 3 × 100 μL of phosphate buffered saline solution. gA containing tBLMs were created by predissolving 100 nM gA into the ethanolic mobile 3 mM lipid phase solution.[7,19]

Val-containing tBLMs were prepared by incubating the membranes with 100 μL of 100 μM Val in electrolyte solution containing either 1 mM KCl or 1 mM KCl with 100 mM NaCl for 15 min and then washed with Val-free electrolyte solutions (3 × 100 μL).

The ac impedance spectroscopy measurements were performed using a laboratory built swept frequency impedance spectrometer employing a 30 mV peak-to-peak ac excitation at 0.1, 0.2, 0.5, 1, 2, 5, 40, 100, 200, 500, and 1000 Hz. Fixed dc biases in the range ±300 mV were applied and left for 5 min prior to measurement in order to fully charge C_{th} and accommodate any equilibration effects arising from the restricted ionic diffusion within the reservoir space.

As an example of the lack of intrinsic voltage dependence of gA, its conduction was measured by applying dc voltage transients across the tethered membranes (Figure 4A) using an eDAQ ER466 integrated potentiostat in conjunction with eScope software (eDAQ Pty Ltd., Australia) operating with a bandwidth of 100 kHz, as described previously.[6] Rectangular voltages pulses of 20 ms duration, increasing from 0 to ±50 mV, were applied. Simultaneous current−voltage recordings at 2 ms were averaged over 16 sweeps with a repetition delay of 1 s. The measurement at 2 ms is well within the decay time of the transmembrane potential dominated by the tethering gold capacitance (C_{th}) and the total membrane conduction, G_m, where $G_m = G_i + G_b$. Potentials are defined as that of the tethered gold electrode relative to the counter electrode.

The electrical impedance spectroscopy data obtained for tBLMs with and without gA were interpreted using the equivalent circuit shown in Figure 1B. The data were fitted to G_m, R_{PBS}, and C_{th} where C_{th} was further modeled using a constant phase element (CPE). A Monte Carlo fitting routine sought minimal RMS differences between experimental data and an analytical solution to the equivalent circuit. The derived values of G_m for bias potentials of +300, 0, and −300 mV, with and without gA, are shown in Figure 3.

RESULTS AND DISCUSSION

Interpretation of Bode Plots. Bode plots (Figure 2) are a convenient measure for modeling the impedance properties of channels and carriers and are presented as (A) a plot of the log of the impedance magnitude with respect to the logarithm of the excitation frequency and (B) a plot of the phase angle between the excitation potential and the resultant current with respect to the logarithm of the excitation frequency.

Impedance Magnitude. From Figure 2A, at low frequencies (0.1−1 Hz) the impedance is dominated by C_{th} and at high frequencies (above 100 Hz) by C_m. At intermediate frequencies the dominant feature is the conduction of the membrane G_m.

Phase. That the membrane capacitance and the tethering gold surface capacitance are in series results in a frequency dependency of the phase profile that typically possess a minima at frequencies in the range of 0.1 Hz−1 kHz. The frequency at which this minima occurs ($F_{min}p$) reflects the membrane conductance (assuming only minor changes in membrane capacitance). A higher conductance causes this minimum to shift to higher frequencies and vice versa (Figure 2B). The phase value at minimum phase ($P_{min}p$) reflects the ratio of the capacitance of the tethering gold surface to the membrane capacitance. The greater this ratio, the lower the $P_{min}p$. Assuming

dx.doi.org/10.1021/la504057z | Langmuir XXXX, XXX, XXX−XXX

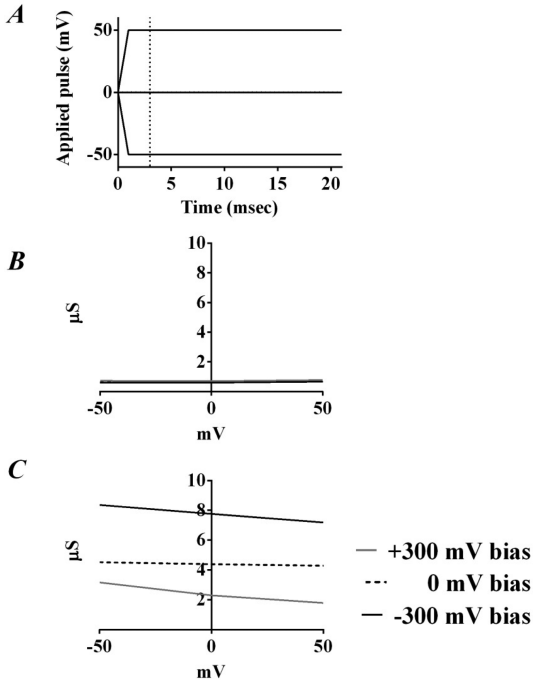

Figure 4. (A) Voltage steps applied to a tBLM containing gA with +300, 0, and −300 mV bias. (B) The resultant membrane conduction as a function of voltage steps in a gA free membrane at these biases as measured 2 ms into each pulse. (C) The same as (B) only in the presence of 100 nM gA. The slopes seen for ±300 mV represent the modulation of the 50 mV pulse on the existing bias, not any intrinsic voltage dependence of gA. These effects are nonlinear with applied voltage as seen in the relatively flat response about zero bias potential.

only minor changes in the membrane capacitance, a higher $P_{min}p$ reflects a smaller tethering capacitance (C_{th}).

Ion Channels: Gramicidin A. *Modeling of Bode Plots.* Figure 3 shows Bode plots for tBLMs with and without gA. In the presence of gA, a negative bias applied between the tethering gold electrode and the counter electrode results in an order of magnitude greater conductance, G_m, than a positive bias. By contrast a control membrane, without gA, showed minimal variation in conduction. However, from the impedance profiles, neither capacitors C_{th} nor C_m were significantly altered by variations in bias potentials in the presence or absence of gA. However, a larger C_{th} was evident in the presence of gA regardless of bias potential.

The calculated conductance values were achieved with better than 3% root mean squared (RMS) agreement with the experimental phase profiles. There was no observable difference in the RMS residuals between the different bias conditions, suggesting that any harmonic distortions or saturating asymmetries in the ac current caused by the bias potential were well below the level of detection. At small excitation levels all responses will appear approximately linear. This will occur even with significant saturation or exhaustion of the reservoir. However, as can be seen in Figure 4C, only small variations in the magnitude of the slope of the G_m-V plot occur in a gA containing membrane employing ±50 mV pulses in the presence of +300 or −300 mV bias. This is only minimally greater than at 0 mV bias.

An approximate calculation of the charge densities controlled by the bias potentials shows they are of the correct order to result in the variation in ionophore conductances observed here. In a typical tethered membrane comprising 90% spacer molecules and 10% tether molecules the reservoir thickness is of order of 2−3 nm.[22] For a phosphate buffered saline of 150 mM NaCl, the ionic density is approximately 9×10^{22} sodium ions per liter, and therefore 9×10^{19} ions cm^{-3} within the 2−3 nm thick reservoir. Thus, the ionic density per unit area is $(4.5-3) \times 10^{13}$ Na^+ ions cm^{-2} or ∼2.8−1.9 μC cm^{-2}. The space filled by the spacer and tether molecules will reduce this number. From the electrical equivalent circuit, the tethering gold capacitance (C_{th}) measured here is of order of 10 μF cm^{-2}; thus, since Q (charge) is equal to $C \times V$ (capacitance × volts), the surface charge at C_{th} due to an applied potential of 300 mV is 3 μC cm^{-2}. That this is comparable and larger indicates that the application of bias voltages well below the oxidation potential of the gold tethering surface can significantly influence the ionic content of the reservoir space and the concentration of ions available for transport across the membrane.

In more detail, the ionic content of the reservoir contributes to both the Stern layer and a diffuse double layer comprising excess ionic charge beyond the Stern layer. Together, these are defined here as C_{th} which is treated as a CPE in the modeling to account for the restricted ionic diffusion. Restricted diffusion will be reflected in an apparent decrease in C_{th} at higher frequencies (resulting in an increase in $P_{min}p$) due to there being insufficient time for a complete charging of C_{th} per cycle of the ac excitation potential. Were the reservoir height expanded substantially beyond this double layer distance, the reservoir electrolyte concentration will trend to that of the bulk electrolyte in which ions of both polarities are matched. This precludes this technique being applied to large volume reservoirs such as exist with patch clamp or classic BLM measurements. The estimated charge stored within a C_{th} of ∼3 μC cm^{-2} indicates an ability of the reservoir space to accommodate sufficient ions to supply a significant current over time without exhausting or saturating the ionic content. For example, for a membrane possessing a ∼1 μS conductance to which 100 mV is applied, 100 nA may be sustained for approximately 40 s before the stored charge will deplete and limit the current.

Pulsed Amperometry. It should be appreciated that the polarity dependence and the cation specificity of an ionophore do not imply that the ionophore itself either is intrinsically rectifying or is voltage-dependent. As mentioned above, Figure 4B shows the membrane conductance, G_m, obtained from measuring the current elicited 2 ms following voltage steps in the range of ±50 mV. In this range G_m is constant, i.e. showing minimal voltage dependence. Above ∼±150 mV a voltage-dependent G_m becomes apparent due to electroporation.[6,23] Though it is evident from Figure 4C that the bias potential controls the average gA conduction, the lack of intrinsic rectification by gA[24] is most clearly evident for low pulsed voltages with zero bias potential.

Ion Carriers: Valinomycin. Figure 5 shows the phase and impedance profiles as a function of frequency (Bode plots) for tBLMs with and without Val with 1 mM K^+, with and without 100 mM Na^+, for bias potentials of +300, 0, and −300 mV.

Impedance. In the absence of Val the impedance versus frequency plots are dominated by the contributions of C_{th} and C_m in series (Figure 5A) and $G_{K^+} + G_{Na^+}$ together with C_{th} and C_m in series (Figure 5B). Altering the bias potential from positive to negative caused minimal change in the impedance profile. However, the introduction of 100 mM Na^+ caused a plateauing of the impedance profile and the appearance of a minimum in the phase profile near 0.5 Hz arising from the nonspecific transport of Na^+ across the membrane. This

dx.doi.org/10.1021/la504057z | Langmuir XXXX, XXX, XXX−XXX

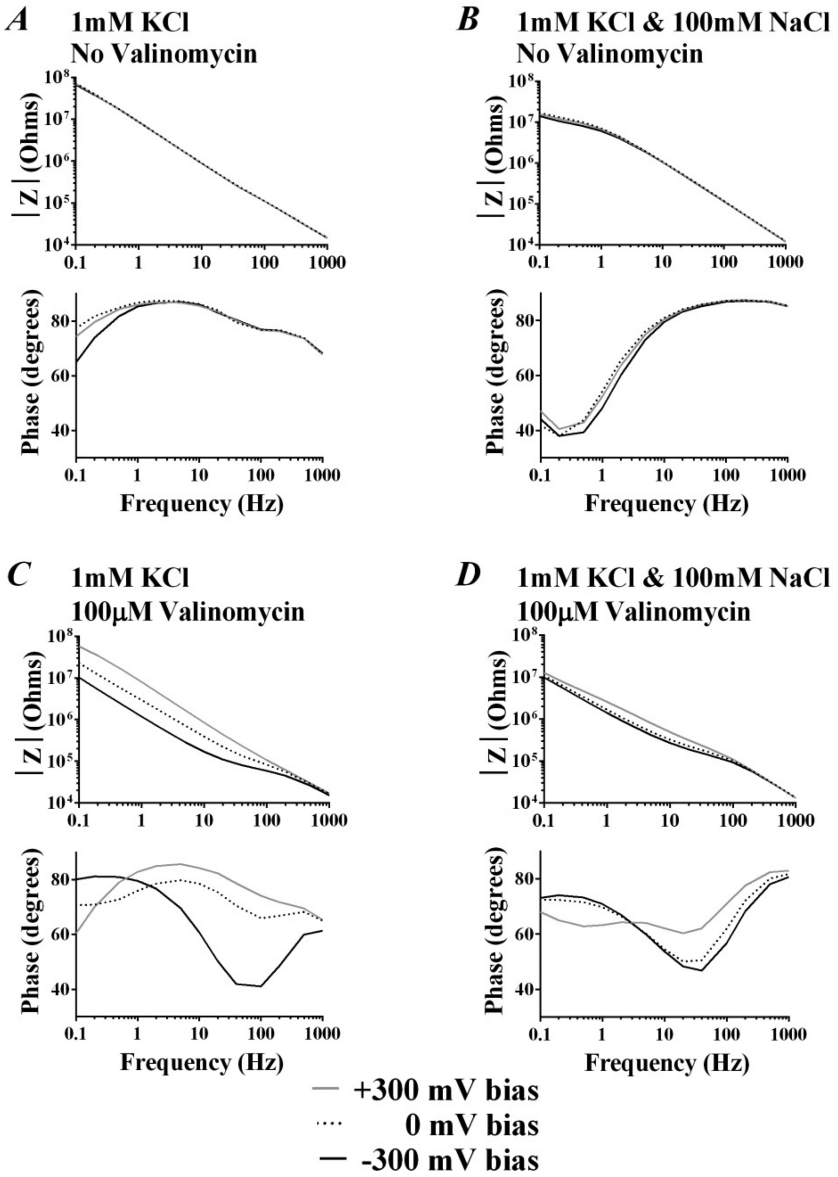

Figure 5. Bode plots for tBLMs without Val (A, B) and with 100 μM Val (C, D) in the presence of +300, 0, and −300 mV biases. Left-hand plots represent tBLMs in the presence of 1 mM K^+, whereas the right-hand plots represent tBLMs in the presence of 1 mM K^+ and 100 mM Na^+.

strongly suggests that such nonspecific Na^+ ion transport is independent of the applied bias polarity.

In the presence of Val and 1 mM K^+ there is a clear dependence on the magnitude and sign of the bias potential at frequencies less than 100 Hz (Figure 5 C,D). This clearly indicates a dependence of C_{th} on bias potential. At frequencies above 500 Hz the traces for +300, 0, and −300 mV converge, indicating that C_m is essentially unaltered.

The inclusion of 100 mM Na^+ in the bathing solution dramatically alters the variation of C_{th}, while minimally influencing C_m. That the sigmoidal transition between the high and low frequency behavior occurs over relatively similar frequencies indicates little variation in G_m under these conditions. This is reflected in the phase profiles where the $F_{min}p$ are similar.

It is also evident from the slope of the impedance profiles below 100 Hz, regardless of bias, that the presence of 100 mM Na^+ in the reservoir space significantly satisfies the charge requirements of C_{th} with minimal supplementary charge being supplied by K^+ ions.

Phase. In the absence of Val the addition of 100 mM Na^+ resulted in a $F_{min}p$ at ∼0.5 Hz, consistent with the nonspecific Na^+ transport across the membrane (Figure 5B). At higher frequencies, in the presence of 100 mM Na^+ the phase trended to 90°, consistent with the profile being dominated by C_m in series with C_{th}. In the presence of only 1 mM K^+ the drooping phase profile at high frequencies reflects additional contributions of R_{K^+} due to the low concentration of the series electrolyte (Figure 5A).

It should be noted that the $F_{min}p$, in the presence of Val and 1 mM K^+ + 100 mM Na^+ (Figure 5D), is ∼50 Hz, compared to ∼0.5 Hz in the absence of Val (Figure 5B). This represents a 100-fold variation in membrane conductance, despite a 100-fold excess of Na^+ concentration, indicating a ∼10000:1 preference of Val for K^+.

In the presence of Val the Na^+ transport predominantly occurs through membrane defects, whereas the K^+ transport occurs predominantly via Val. When modeling such strong ion specificity for an inefficient transporter such as Val, the

dx.doi.org/10.1021/la504057z | *Langmuir* XXXX, XXX, XXX−XXX

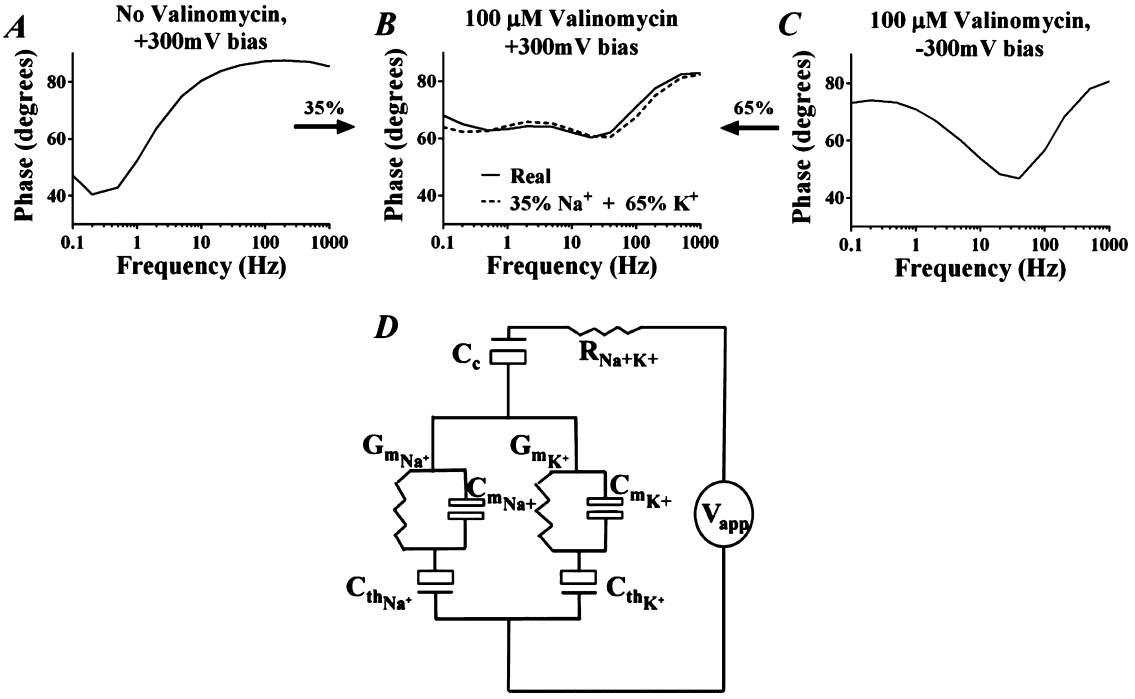

Figure 6. (A) Phase profile of Val free membrane in the presence of 1 mM K^+ and 100 mM Na^+ with +300 mV bias. (B) The same membrane following the addition of 100 μM Val, also at +300 mV bias. Superimposed is a dashed line depicting an arithmetic addition of 35:65 trace (A:C) where (C) is the same membrane following the addition of 100 μM Val at −300 mV bias. (D) is the electrical equivalent circuit of a Val containing membrane bathed in a mixed Na^+K^+ electrolyte solution. Unlike simulations of gA containing membranes, the series tethering capacitance is denoted as C_{th} rather than a CPE because of the relatively inefficient and distributed ion delivery of K^+ by the Val carrier.

elements in the electrical equivalent circuit (Figure 1B) must now be treated as two separated terms (Figure 6D). One describes the favored ion transport, and a second describes the less favored, essentially background, conduction. In the presence of a −300 mV bias the phase profile is dominated by the Val transport; however, as the bias is switched to 0 and +300 mV a more complex relationship becomes evident; in particular at +300 mV two phase minima appear, the first at ∼0.5 Hz and the second at ∼50 Hz (Figure 5D). The former is identified with Na transport, and the latter with K^+ transport. This interpretation is supported by Figure 6, which describes a simple addition of the Val free control phase profile at +300 mV bias (Figure 6A) with the phase profile of a −300 mV bias Val containing membrane, Figure 6C (all bathed in 1 mM K^+ and 100 mM Na^+). As can be seen, a 35:65 additive combination of these two spectra closely resembles the experimental data obtained with +300 mV bias in the presence of Val (Figure 6B). This effect is explained by reference to the equivalent circuit depicted in Figure 6D in which two C_m, G_m, C_{th} networks describe the response to the Na^+ and, separately, the K^+ ionic populations.

SUMMARY

The effect of the bias potential reveals the limiting process for K^+ transport by Val is the Val concentration, whereas the limiting process for cation transport by gA is the cation concentration. In the case of gA conduction, this is reflected by a shift in $F_{min}p$ at essentially constant $P_{min}p$ and, in the case of Val, by a shift in $P_{min}p$ at essentially constant $F_{min}p$. For gA, the ion flux is sufficiently high to average all conduction pathways to a single value of G_m and thus $F_{min}p$. In this case, $P_{min}p$ slightly increases at high $F_{min}p$, reflecting restricted cationic diffusion within the reservoir space. For Val, the ion flux is far less efficient, being only a single K^+ transported per Val passage across the membrane. This results in both a Val concentration limit to conduction and a separately evident phase minima arising from the nonspecific Na^+ conduction through the membrane.

For gA, a high flux of ions enters at well-separated localized points in the membrane. This requires a relatively slow radial diffusion by the ions away from the ion channel to populate the tethering capacitance (C_{th}). This introduces a resistive phase contribution to the tethering capacitance conveniently described by employing a CPE. However, for Val, the K^+ ions are delivered singly with an even distribution across the membrane, resulting in a more nearly capacitive property for the tethering capacitance (C_{th}).

The nanoscale separation of tethered membranes from their supporting surface permits the local ionic environment to be modified though the application of fixed bias potentials. The reservoir ion sequestration technique (RIS), described here, raises the concentration of the ion complementary to the charge polarity applied to the electrode. This provides a convenient tool to determine (i) the preferred polarity of the ionophore conductance, (ii) the intrinsic voltage dependency or the rectifying properties of the ionophore, and (iii) the differences between the rate limiting transport, such as exists for carriers, and ion concentration limited transport such as exists for channels.

AUTHOR INFORMATION

Corresponding Author

*E-mail: charles.cranfield@uts.edu.au (C.G.C.).

Notes

The authors declare the following competing financial interest(s): We declare that Bruce Cornell is a shareholder of Surgical Diagnostics Pty Ltd.

dx.doi.org/10.1021/la504057z | *Langmuir* XXXX, XXX, XXX−XXX

■ ACKNOWLEDGMENTS

This study was supported by National Health & Medical Research Council (NH&MRC) of Australia (Grant 635525) and ARC Linkage grant (LP120200078). Bruce Cornell is a shareholder of Surgical Diagnostics Pty Ltd., and Taren Bettler is a student volunteer researcher at Surgical Diagnostics Pty Ltd. We also acknowledge Sonia Carne's technical support and Paul Duckworth for his insightful discussions.

■ REFERENCES

(1) Benz, R.; Läuger, P. Kinetic analysis of carrier-mediated ion transport by the charge-pulse technique. *J. Membr. Biol.* **1976**, *27* (1), 171−191.
(2) Merzlyak, P. G.; Capistrano, M.-F. P.; Valeva, A.; Kasianowicz, J. J.; Krasilnikov, O. V. Conductance and ion selectivity of a mesoscopic protein nanopore probed with cysteine scanning mutagenesis. *Biophys. J.* **2005**, *89* (5), 3059−3070.
(3) Jackman, J.; Knoll, W.; Cho, N.-J. Biotechnology applications of tethered lipid bilayer membranes. *Materials* **2012**, *5*, 2637−2657.
(4) McGillivray, D. J.; Valincius, G.; Heinrich, F.; Robertson, J. W. F.; Vanderah, D. J.; Febo-Ayala, W.; Ignatjev, I.; Lösche, M.; Kasianowicz, J. J. Structure of functional staphylococcus aureus α-hemolysin channels in tethered bilayer lipid membranes. *Biophys. J.* **2009**, *96* (4), 1547−1553.
(5) Raguse, B.; Braach-maksvytis, V.; Cornell, B. A.; King, L. G.; Osman, P. D. J.; Pace, R. J.; Wieczorek, L. Tethered lipid bilayer membranes: Formation and ionic reservoir characterization. *Langmuir* **1998**, *7463*, 648−659.
(6) Cranfield, C. G.; Cornell, B. A.; Grage, S. L.; Duckworth, P.; Carne, S.; Ulrich, A. S.; Martinac, B. Transient potential gradients and impedance measures of tethered bilayer lipid membranes: Pore-forming peptide insertion and the effect of electroporation. *Biophys. J.* **2014**, *106*, 182−189.
(7) Krishna, G.; Schulte, J.; Cornell, B. A.; Pace, R. J.; Osman, P. D. Tethered bilayer membranes containing ionic reservoirs: selectivity and conductance. *Langmuir* **2003**, *19* (6), 2294−2305.
(8) Valincius, G.; Meškauskas, T.; Ivanauskas, F. Electrochemical impedance spectroscopy of tethered bilayer membranes. *Langmuir* **2012**, *28*, 977−90.
(9) Hotchkiss, R. D.; Dubos, R. J. Fractionation of the bactericidal agent from cultures of a soil bacillus. *J. Biol. Chem.* **1940**, *132* (2), 791−792.
(10) O'Connell, A. M.; Koeppe, R. E.; Andersen, O. S. Kinetics of gramicidin channel formation in lipid bilayers: transmembrane monomer association. *Science* **1990**, *250* (4985), 1256−1259.
(11) Wallace, B. Recent advances in the high resolution structures of bacterial channels: gramicidin A. *J. Struct. Biol.* **1998**, *121* (2), 123−141.
(12) Ketchem, R.; Hu, W.; Cross, T. High-resolution conformation of gramicidin A in a lipid bilayer by solid-state NMR. *Science* **1993**, *261* (5127), 1457−1460.
(13) Urry, D. The gramicidin A transmembrane channel: a proposed π (L, D) helix. *Proc. Natl. Acad. Sci. U. S. A.* **1971**, *68* (3), 672−676.
(14) Arseniev, A.; Barsukov, I.; Bystrov, V.; Lomize, A.; Ovchinnikov, Y. A. H-NMR study of gramicidin A transmembrane ion channel: Head-to-head right-handed, single-stranded helices. *FEBS Lett.* **1985**, *186* (2), 168−174.
(15) Smart, O. S.; Goodfellow, J. M.; Wallace, B. The pore dimensions of gramicidin A. *Biophys. J.* **1993**, *65* (6), 2455−2460.
(16) Finkelstein, A.; Andersen, O. S. The gramicidin A channel: a review of its permeability characteristics with special reference to the single-file aspect of transport. *J. Membr. Biol.* **1981**, *59* (3), 155−171.
(17) Hladky, S.; Haydon, D. Ion transfer across lipid membranes in the presence of gramicidin A: I. Studies of the unit conductance channel. *Biochim. Biophys. Acta, Biomembr.* **1972**, *274* (2), 294−312.
(18) Becucci, L.; Innocenti, M.; Salvietti, E.; Rindi, A.; Pasquini, I.; Vassalli, M.; Foresti, M. L.; Guidelli, R. Potassium ion transport by gramicidin and valinomycin across a Ag (111)-supported tethered bilayer lipid membrane. *Electrochim. Acta* **2008**, *53* (22), 6372−6379.
(19) Cornell, B. a.; Braach-Maksvytis, V. L.; King, L. G.; Osman, P. D.; Raguse, B.; Wieczorek, L.; Pace, R. J. A biosensor that uses ion-channel switches. *Nature* **1997**, *387*, 580−3.
(20) Kozuch, J.; Steinem, C.; Hildebrandt, P.; Millo, D. Combined electrochemistry and surface-enhanced infrared absorption spectroscopy of gramicidin A incorporated into tethered bilayer lipid membranes. *Angew. Chem., Int. Ed.* **2012**, *51* (32), 8114−8117.
(21) Pinkerton, M.; Steinrauf, L.; Dawkins, P. The molecular structure and some transport properties of valinomycin. *Biochem. Biophys. Res. Commun.* **1969**, *35* (4), 512−518.
(22) Heinrich, F.; Ng, T.; Vanderah, D. J.; Shekhar, P.; Mihailescu, M.; Nanda, H.; Lösche, M. A new lipid anchor for sparsely tethered bilayer lipid membranes. *Langmuir* **2009**, *25*, 4219−29.
(23) Hoiles, W.; Krishnamurthy, V.; Cranfield, C. G.; Cornell, B. An engineered membrane to measure electroporation: Effect of tethers and bioelectronic interface. *Biophys. J.* **2014**, *107* (6), 1339−1351.
(24) Busath, D.; Szabo, G. Permeation characteristics of gramicidin conformers. *Biophys. J.* **1988**, *53* (5), 697−707.